

Nuclear suppression of the ϕ meson yields with large p_T at the RHIC and the LHC

Wei Dai^{1,a}, Xiao-Fang Chen², Ben-Wei Zhang^{1,b}, Han-Zhong Zhang¹, Enke Wang¹

¹ Key Laboratory of Quark and Lepton Physics (MOE) and Institute of Particle Physics, Central China Normal University, Wuhan 430079, China

² School of Physics and Electronic Engineering, Jiangsu Normal University, Xuzhou 221116, China

Received: 6 February 2017 / Accepted: 9 August 2017 / Published online: 28 August 2017

© The Author(s) 2017. This article is an open access publication

Abstract We calculate ϕ meson transverse momentum spectra in p+p collisions as well as their nuclear suppressions in central A + A collisions both at the RHIC and the LHC in LO and NLO with the QCD-improved parton model. We have included the parton energy loss effect in a hot/dense QCD medium with the effectively medium-modified ϕ fragmentation functions in the higher-twist approach of jet quenching. The nuclear modification factors of the ϕ meson in central Au + Au collisions at the RHIC and central Pb + Pb collisions at the LHC are provided, and nice agreement of our numerical results at NLO with the ALICE measurement is observed. Predictions of the yield ratios of neutral mesons such as ϕ/π^0 , ϕ/η and ϕ/ρ^0 at large p_T in relativistic heavy-ion collisions are also presented for the first time.

1 Introduction

The jet quenching phenomenon [1], as one of the key discoveries made so far in relativistic heavy-ion collisions (HIC) at the RHIC and the LHC, has been extensively studied for a wide range of observables. Among them, the yield suppression of the produced final-state hadrons at large transverse momentum p_T [2] provides the most direct and one of the fundamental observables which can reveal the mechanism of parton energy loss in a dense QCD medium and test many-body QCD theory. Experimentally, a suppression of approximately same magnitude is observed for π^0 , η and ρ^0 productions at the RHIC despite their different masses [3–5], and a similar observation has also been made by the ALICE Collaboration [6]. By considering the fast parton suffers medium-induced energy loss while propagating through the QCD medium before its fragmenting into final-state hadrons in the vacuum outside the QCD medium, we explore the suppres-

sion pattern of these neutral mesons with the next-to-leading order (NLO) calculations in the QCD-improved parton model in the previous publications [7–10]. It has been demonstrated that, for productions of π^0 , η and ρ^0 mesons containing light valence quark, quark fragmentation gives the largest contributions at large p_T ; with the relatively weak p_T and z_h (momentum fraction of partons carried by the fragmented hadrons) dependence of their quark fragmentation functions (FFs), even though the jet quenching effect will alter the gluon and quark relative contributions to the yields of these neutral mesons in HIC relative to p + p collisions, the η/π^0 and ρ^0/π^0 ratios in HIC will eventually coincide with p + p at very large p_T [9, 10].

In this paper, we apply the same framework to investigate the $\phi(s\bar{s})$ meson, which is also a light meson but contains strange (anti-strange) valence quarks. The production of the ϕ meson can be used to probe different aspects of the heavy-ion collisions, such as the strangeness enhancement and chiral symmetry restoration. Here, we focus on parton energy loss effect on the ϕ meson cross section at large p_T and its nuclear modification factor to further examine the particle species dependence of jet quenching in the QCD medium. We notice that due to the lack of precise parametrizations of the fragmentation functions of the ϕ meson, theoretical calculations of the ϕ meson production at large p_T in either p + p collisions or HIC at the RHIC and the LHC have not been available so far.

To make a perturbative QCD calculation of ϕ production at large transverse momentum, the parton FFs of the ϕ meson $D_{q,g\rightarrow\phi}(z_h, Q)$ at any hard scale Q should be needed. In our study we utilize the availability of a broken SU(3) model description of vector meson productions [11, 12] to have an initial parametrization of ϕ FFs in vacuum at a starting energy scale $Q_0^2 = 1.5 \text{ GeV}^2$ as an input. We calculate the productions of the ϕ meson in p + p collision at $\sqrt{s_{NN}} = 200 \text{ GeV}$ and $\sqrt{s_{NN}} = 2.76 \text{ TeV}$ up to NLO, and find the theoretical results to be in good agreement with the PHENIX and

^a e-mail: davidwillcn2008@gmail.com

^b e-mail: bwzhang@mail.ccnucnu.edu.cn

ALICE data, respectively. Then we numerically investigate the ϕ meson productions in A + A collisions by incorporating the effectively medium-modified FFs in the higher-twist approach of parton energy loss. We provide for the first time the numerical results of the ϕ meson yields in central A + A collisions both at the RHIC and the LHC. We confront the theoretical results of the nuclear modification factor $R_{AA}(\phi)$ in Pb + Pb collisions at LHC with the existing experimental data by the ALICE Collaboration, and find they match well with each other. We may explore further how the change of jet chemistry due to partonic energy loss results in different suppression patterns between $\phi(s\bar{s})$ meson and other neutral mesons such as π^0 , η and ρ^0 by plotting the yield ratios of ϕ/π^0 , ϕ/η and ϕ/ρ^0 in p + p and in HIC.

2 Large p_T yield of the ϕ meson in p + p

The leading hadron production in p + p collisions can be factorized into three parts as parton distribution functions (PDFs) inside the incoming protons, elementary partonic scattering cross sections $d\hat{\sigma}/d\hat{t}$, and parton FFs to the final-state hadron [14]. To facilitate the discussions of parton FFs in vacuum and medium, we take the following formula:

$$\frac{1}{p_T} \frac{d\sigma_h}{dp_T} = \int F_q \left(\frac{p_T}{z_h} \right) \cdot D_{q \rightarrow h}(z_h, Q^2) \frac{dz_h}{z_h^2} + \int F_g \left(\frac{p_T}{z_h} \right) \cdot D_{g \rightarrow h}(z_h, Q^2) \frac{dz_h}{z_h^2}. \quad (1)$$

One can see the single hadron production in p + p collision will be determined by two factors: the initial hard (parton-) jet spectrum $F_{q,g}(p_T)$ and the parton FFs $D_{q,g \rightarrow h}(z_h, Q^2)$ to the final-state hadron. In our calculations, we employed CTEQ6M parametrization for PDFs [15] in colliding protons, which has been convoluted with partonic scattering cross sections $d\hat{\sigma}/d\hat{t}$ to obtain $F_{q,g}(p_T)$. $D_{q,g \rightarrow h}(z_h, Q^2)$ denotes the parton FFs in vacuum, which give the possibilities of scattered parton fragmenting into hadron h at momentum fraction z_h and fragmentation scale Q . In practice, the factorization, renormalization and fragmentation scales are usually chosen to be the same and proportional to the final-state p_T of the leading hadron.

Due to the paucity of the experimental data, there are few parameterized ϕ parton FFs. Recently a broken $SU(3)$ model is proposed to extracting parton FFs of the vector mesons [11,12]. The complexity of the meson octet fragmentation functions has been reduced considerably by introducing the $SU(3)$ flavor symmetry with a symmetry breaking parameter. The isospin and charge conjugation invariance of the vector mesons further reduce the independent quark flavor FFs into functions named valence (V) and sea (γ). The inputs of valence $V(x, Q_0^2)$, sea $\gamma(x, Q_0^2)$ and gluon $D_g(x, Q_0^2)$ FFs

are parameterized into a standard polynomial at a starting low energy scale of $Q_0^2 = 1.5 \text{ GeV}^2$ such as

$$F_i(x) = a_i x^{b_i} (1-x)^{c_i} (1+d_i x + e_i x^2). \quad (2)$$

In addition, since the ϕ meson is dominated by its $s\bar{s}$ component, the FFs can be expressed as orthogonal combinations of the $SU(3)$ octet (ω_8) and singlet (ω_1) states:

$$\phi = \cos \theta \omega_8 - \sin \theta \omega_1. \quad (3)$$

And a few additional parameters such as f_1^u, f_1^s, f_{sea} , representing the singlet constants and the sea suppression, the vector mixing angle θ mentioned in the above equation are introduced. Together with the three sets of parameters in $V(x, Q_0^2), \gamma(x, Q_0^2)$ and $D_g(x, Q_0^2)$, all these parameters are initially parameterized at starting scale of $Q^2 = 1.5 \text{ GeV}^2$ by evolving through the DGLAP equation [13], then fitting the cross section at NLO with the measurements of LEP (ρ, ω) and SLD (ϕ, K^*) at $\sqrt{s} = 91.2 \text{ GeV}$. The parameters for ϕ FFs in vacuum at $Q^2 = 1.5 \text{ GeV}^2$ are listed in Refs. [11,12] and we obtain the ϕ meson FFs at any energy scale Q by evolving them in the numerical DGLAP equation at NLO [13].

To understand the pure $s\bar{s}$ state nature of ϕ and its influence to the production, we plot in Fig. 1 the initial parameterized FFs at initial energy scale $Q^2 = 1.5 \text{ GeV}^2$ (left panel) and the DGLAP evolved FFs at $Q^2 = 100 \text{ GeV}^2$ (right panel). It is observed that $D_{s \rightarrow \phi}(z_h, Q) \gg D_{u \rightarrow \phi}(z_h, Q)$, and in the intermediate and large z_h regions gluon FF to ϕ meson is much larger than up (down) quark FFs to ϕ . We notice that these features are quite different from FFs of other neutral mesons (such as ρ^0 [10]) where up (down) quark FFs are much larger than strange quark FFs. In Fig. 2 we show the

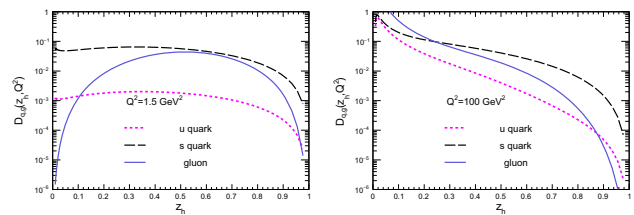


Fig. 1 Parton FFs of the ϕ meson as a function of z_h at the initial scale $Q^2 = 1.5 \text{ GeV}^2$ (left panel), and at the scale of $Q^2 = 100 \text{ GeV}^2$ (right panel)

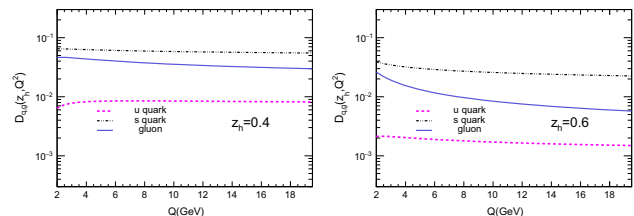


Fig. 2 Left ϕ FFs as a function of the scale Q at $z_h = 0.6$; right ϕ FFs as a function of the scale Q at $z_h = 0.6$

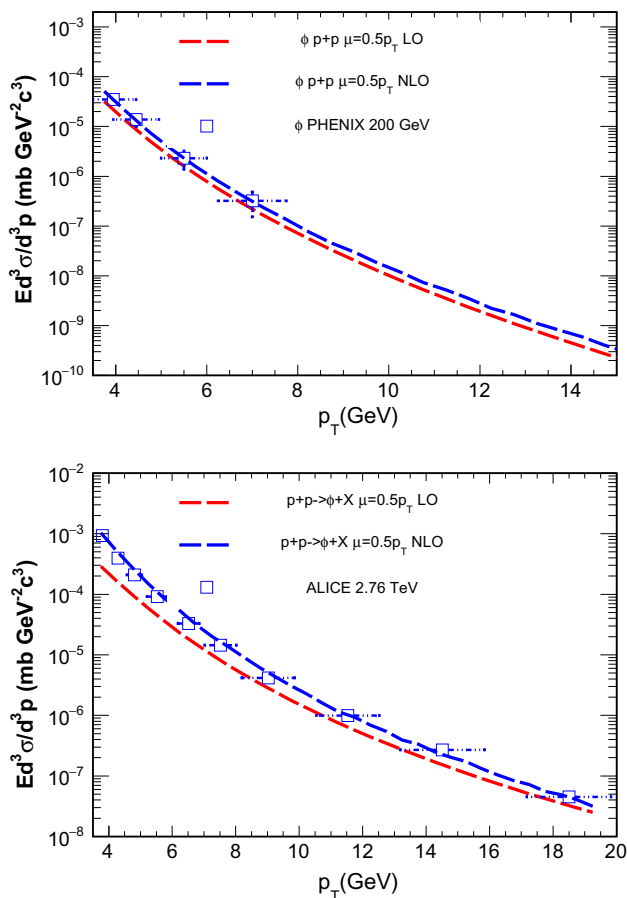


Fig. 3 *Top* Numerical calculation of the ϕ production in p+p collisions with $\sqrt{s_{NN}} = 200$ GeV at the RHIC with STAR data [16] ($\sigma_{NN} = 42$ mb). *Bottom* Numerical calculation of the ϕ production in p + p collisions with $\sqrt{s_{NN}} = 2.76$ TeV at the LHC with ALICE data [17, 18] ($\sigma_{NN} = 65$ mb [19])

$Q(p_T)$ dependence of the ϕ meson FFs at different fixed z_h . We can see in the plotted Q region $D_{s \rightarrow \phi}(z_h, Q) > D_{g \rightarrow \phi}(z_h, Q) \gg D_{u \rightarrow \phi}(z_h, Q)$. Because in the initial hard scattering processes more gluon partons will be produced than strange quarks we may expect that there will be competition between strange quark and gluon fragmented contributions of the ϕ meson yield in p + p collisions.

With the availability of ϕ FFs in vacuum, we make a perturbative calculation of the ϕ meson p_T distribution in elementary proton–proton collisions at $\sqrt{s_{NN}} = 200$ GeV and $\sqrt{s_{NN}} = 2.76$ TeV with the QCD-improved parton model. In Fig. 3 we confront the numerical simulations at LO and NLO with the experimental data of the ϕ production in p + p collision at the RHIC by STAR [16] (top panel), and the LHC by ALICE [18] (bottom panel). One can see the NLO results with factorization and normalization scales $\mu = 0.5p_T$ give very nice description of data on ϕ cross section in p + p. In the following calculations the same hard scales $\mu = 0.5p_T$ will be adopted.

3 Large p_T yield of the ϕ meson in HIC

To study the single hadron productions in high-energy nuclear collisions, we have utilized the generalized factorization of twist-four processes to calculate parton energy loss due to medium-induced gluon radiation of a hard partons passing through the hot/dense QCD medium, and we derive the effectively medium-modified fragmentation functions in the higher-twist approach of parton energy loss [20–24]. The effectively medium-modified FFs, which have been effectively taken into account partonic energy loss effect, and which have been used in the numerical simulations of leading hadron productions in A + A collisions, are written as [7–10]

$$\begin{aligned} \tilde{D}_q^h(z_h, Q^2) &= D_q^h(z_h, Q^2) + \frac{\alpha_s(Q^2)}{2\pi} \int_0^{Q^2} \frac{d\ell_T^2}{\ell_T^2} \\ &\times \int_{z_h}^1 \frac{dz}{z} \left[\Delta\gamma_{q \rightarrow qg}(z, x, x_L, \ell_T^2) D_q^h\left(\frac{z_h}{z}\right) \right. \\ &\left. + \Delta\gamma_{q \rightarrow gq}(z, x, x_L, \ell_T^2) D_g^h\left(\frac{z_h}{z}\right) \right]. \end{aligned} \quad (4)$$

They take a similar form to the vacuum bremsstrahlung corrections leading to the DGLAP evolution for FFs in vacuum, with the vacuum splitting functions replaced by the medium-modified splitting functions $\Delta\gamma_{q \rightarrow qg}$ and $\Delta\gamma_{q \rightarrow gq}$. Therefore, to calculate the production of leading hadrons in A + A collisions at the NLO, we utilize the NLO partonic cross sections in the same way as in p+p and the NLO nuclear PDFs, which are then convoluted with an effective medium-modified fragmentation function given by Eq. (4), where the vacuum FFs are evolved with the NLO DGLAP equation, while the correction convolutes a medium-induced kernel with the (DGLAP) evolved FFs at scale Q^2 . The medium-modified splitting functions depend on the twist-four quark–gluon correlations inside the medium $T_{qg}^A(x, x_L)$, as demonstrated by [20–22]:

$$\begin{aligned} \Delta\gamma_{q \rightarrow qg}(z, x, x_L, \ell_T^2) &= \left[\frac{1+z^2}{(1-z)_+} T_{qg}^A(x, x_L) + \delta(1-z) \right. \\ &\left. \times \Delta T_{qg}^A(x, x_L) \right] \frac{2\pi\alpha_s C_A}{\ell_T^2 N_c f_q^A(x)}; \end{aligned} \quad (5)$$

$$\Delta\gamma_{q \rightarrow gq}(z, x, x_L, \ell_T^2) = \Delta\gamma_{q \rightarrow qg}(1-z, x, x_L, \ell_T^2). \quad (6)$$

This is due to the fact that the twist-four quark–gluon correlations $T_{qg}^A(x, x_L)$, which depend on the properties of the medium, cannot be determined directly by the theoretical calculation. By assuming a thermal ensemble of quasi-particle states in the hot and dense medium, and also neglecting the multiple particle correlations inside the hot medium, we may find the quark–gluon correlation function in the higher-twist approach to multiple scattering in the QCD medium factorized as [7–10, 25]

$$\frac{T_{qg}^A(x, x_L)}{f_q^A(x)} = \frac{N_c^2 - 1}{4\pi\alpha_s C_R} \frac{1+z}{2} \int dy^- 2 \sin^2 \left[\frac{y^- \ell_T^2}{4Ez(1-z)} \right] \times [\hat{q}_R(E, x_L, y) + c(x, x_L) \hat{q}_R(E, 0, y)]. \quad (7)$$

Considering the contribution of the radiative energy loss and assuming $x \gg x_L, x_T$, we will have the jet transport parameter $\hat{q}_R(E, y) \equiv \hat{q}_R(E, x_L, y) \approx \hat{q}_R(E, 0, y)$. Phenomenologically given the evolutionary space and time profile to the jet transport parameter $\hat{q}_R(E, y)$, one can finally calculate the effective medium-modified quark fragmentation function according to Eq. (4). The space-time evolution of the medium phenomenological is introduced by the value of the jet transport parameter \hat{q} relative to the initial value q_0 , located at the center of the overlap region at the initial time of the QGP formation. We note that the treatment here is model-dependent and a satisfactory treatment of medium modifications of parton fragmentation from first principles is still needed. To consider the radial flow, we also include the product of the four momentum of the jet and the four flow velocity of the medium along the jet propagation path in the collision frame [8].

The total energy loss embodied in the medium-modified quark fragmentation function is in the energies carried away by the radiative gluon (reflected by the medium-modified splitting functions):

$$\frac{\Delta E}{E} = \frac{2N_c\alpha_s}{\pi} \int dy^- dz d\ell_T^2 \frac{1+z^2}{\ell_T^4} \times \left(1 - \frac{1-z}{2}\right) \hat{q}(E, y) \sin^2 \left[\frac{y^- \ell_T^2}{4Ez(1-z)} \right], \quad (8)$$

which is also proportional to the jet transport parameter \hat{q} .

A full three-dimensional (3+1D) ideal hydrodynamics description [26,27] is employed to give the space-time evolutionary information of the QCD medium such as the parton density, temperature, the fraction of the hadronic phase and the four flow velocity at every time step. There remains only one parameter $\hat{q}_0\tau_0$: the product of the initial value of jet transport parameter \hat{q}_0 at the most central position in the overlap region and the initial time τ_0 , when the QCD medium is formed. It characterizes the overall strength of the jet-medium interaction relying on the collision energy and system, also the amount of the energy loss of the energetic jets. To finally derive the production in A + A collisions, we replace the vacuum fragmentation functions in Eq. (1) by the initial production position and the jet propagation direction averaged medium-modified fragmentation functions, scaled by the number of binary nucleon-nucleon collisions at the average value of the impact parameter b in A + A collisions. To demonstrate the medium modification of the single hadron production, the nuclear modification factor R_{AA} as a func-

tion of p_T is introduced to divide cross sections in A + A collisions by the ones in p+p, scaled by the number of binary nucleon-nucleon collisions with a chosen impact parameter b as follows:

$$R_{AB}(b) = \frac{d\sigma_{AB}^h/dy d^2p_T}{N_{bin}^{AB}(b) d\sigma_{pp}^h/dy d^2p_T}, \quad (9)$$

where $N_{bin}^{AB}(b) = \int d^2r t_A(r) t_B(|\mathbf{b} - \mathbf{r}|)$ is calculated using the Glauber model. The fixed values of the impact parameters in the calculation of the spectra and the modification factor are also determined through the Glauber geometric fractional cross sections at given centrality of the heavy-ion collisions.

We calculate the inclusive ϕ meson productions in nuclear collisions up to NLO at the RHIC and the LHC using this unified framework as studying π^0 , η and ρ^0 [7–10]. We apply the same choice of the parameter values $\hat{q}_0\tau_0$ with the initial formation time $\tau_0 = 0.6$ fm of the quark-gluon plasma, which has been found to give very nice descriptions of those neutral mesons in HIC. Initial-state cold nuclear matter effects are also taken into account by employing the EPS09s parametrization set of nuclear PDFs $f_{a/A}(x_a, \mu^2)$ [28].

4 Results and discussions

In the numerical calculations, the extraction of the quark jet transport coefficient \hat{q}_0 at the central of the most central A + A collisions at a given initial time τ_0 is performed by best fitting to the PHENIX data on π^0 production spectra in 0–5% Au + Au collisions at $\sqrt{s} = 200$ GeV, which gives $\hat{q}_0 = 1.20 \pm 0.30$ GeV²/fm, and also fitting to the ALICE and CMS data combined on charged hadron spectra in 0–5% Pb + Pb collisions at $\sqrt{s} = 2.76$ TeV, which gives $\hat{q}_0 = 2.2 \pm 0.5$ GeV²/fm at $\tau_0 = 0.6$ fm/c [8,9]. As already mentioned in Ref. [29], it is consistent with the assumption that the jet transport coefficient is proportional to the initial parton density or the transverse density of charged hadron multiplicity in midrapidity. The charged hadron pseudorapidity density at midrapidity $dN_{ch}/d\eta \approx 1584$ in the most central 0–5% Pb + Pb collisions at $\sqrt{s} = 2.76$ TeV is 2.3 ± 0.24 larger than $dN_{ch}/d\eta \approx 687$ in 0–5% Au + Au collisions at $\sqrt{s} = 200$ GeV. Also the ratio of the transverse hadron density in central Pb + Pb collisions at the LHC to that in Au + Au at RHIC is about 2.2 ± 0.23 , which is also very close to the value of the ratio of $\hat{q}_0^{\text{LHC}}/\hat{q}_0^{\text{RHIC}} \approx 1.83$.

We firstly confront our calculation with the existing experimental data by the ALICE Collaboration [17,18] in the top panel of Fig. 4, and we show R_{AA} as a function of p_T in Pb + Pb collisions at LHC calculated in NLO by choosing $q_0\tau_0 = 1.32$ GeV² with $\tau_0 = 0.6$ fm. The NLO results of the R_{AA} agree very well with the ALICE data, which varies between 4–20 GeV. In the bottom panel of Fig. 4 we

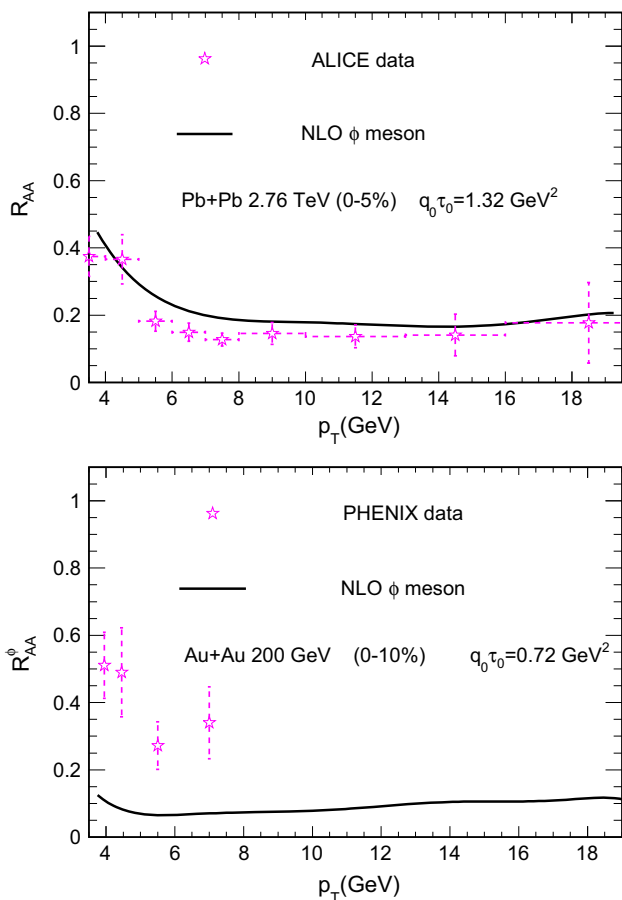


Fig. 4 Top The nuclear modification factor as a function of p_T in Pb + Pb collisions at the LHC calculated at both LO and NLO accuracy, with ALICE data [17, 18]. Bottom The nuclear modification factor as a function of p_T in Au + Au collisions at the RHIC calculated at both LO and NLO accuracy, with PHENIX data [16]

present numerical predictions of R_{AA} in Au + Au collisions at the RHIC both at NLO with the jet transport parameter $q_0\tau_0 = 0.72 \text{ GeV}^2$ ($\tau_0 = 0.6 \text{ fm}$), where PHENIX data [16] available for a rather limited p_T region (4–7 GeV) are also shown. Our theoretical prediction in Fig. 4 (bottom) undershoots the experimental data. In this manuscript, the pQCD-based calculation is better applicable at the larger p_T region; other non-perturbative mechanisms such as recombination in the $p_T = 2\text{--}8 \text{ GeV}$ region is also not included.

We note that ϕ meson production has a unique feature as compared to productions of other neutral mesons (π^0 , η and ρ^0). In the top panel of Fig. 5 we plot the only gluon (strange quark) fragmentating contribution fraction of the ϕ yield in p + p collision at the RHIC. We find though that in the quark model the ϕ meson is in the $s\bar{s}$ state, the strange quark fragmentation only gives a 5–10% contribution of the total ϕ meson yield, and the dominant contribution to the total ϕ meson yield comes from gluon fragmentation in the wide range of p_T (even at the region $p_T \sim 20 \text{ GeV}$). This

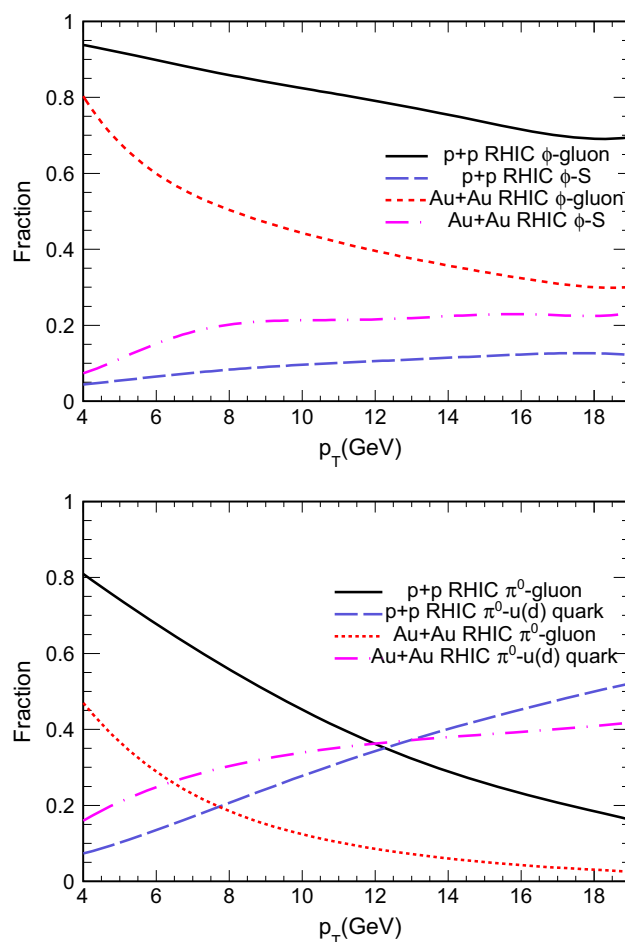


Fig. 5 Gluon and quark contribution fractions of the total ϕ yield (top panel) as well as π^0 yield (bottom panel) in p + p collisions and central Au + Au collisions at the RHIC

feature is in striking contrast with the productions of π^0 , η and ρ^0 . As a comparison in the bottom panel of Fig. 5 we show the only gluon (strange quark) fragmentating contribution fraction of π^0 production in p + p collision at the RHIC. One can observe that the gluon contribution fraction to π^0 goes under 50% when $p_T \sim 9 \text{ GeV}$. At the high p_T region, the π^0 production is dominated by light (up and down) quark contribution, which holds true also for η and ρ^0 production in p + p reactions.

In A + A collisions, the parton energy loss mechanism will change the parton-jet chemistry components because a fast gluon will lose more energy in the QGP than a fast quark due to its large color charge ($\Delta E_g/\Delta E_q = C_A/C_F = 9/4$). Therefore the gluon contribution fraction will be reduced in A + A collisions relative to that in p + p. In Fig. 5 we also provide the parton contribution fraction to the ϕ meson (top panel) and to the π^0 meson (bottom panel) in central Au + Au at the RHIC. The decreasing of the gluon contribution fraction and the increasing of the quark contribution fraction observed in both cases reflect the larger energy loss suffered

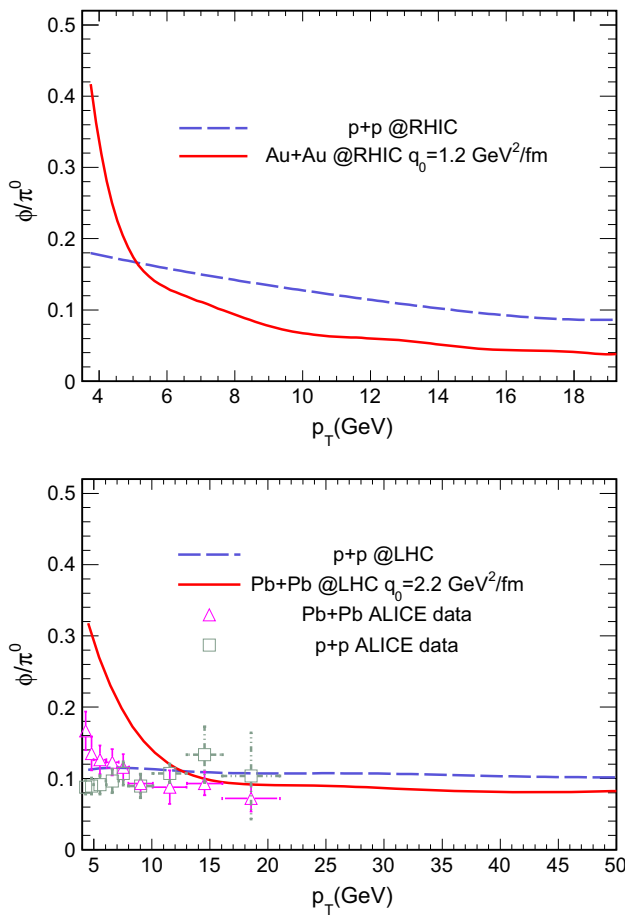


Fig. 6 Top ϕ/π^0 ratio as a function of p_T in p + p and Au + Au collisions at the RHIC. Bottom ϕ/π^0 ratio as a function of p_T in p + p and Pb + Pb collisions at the LHC, comparing with ALICE data [18]

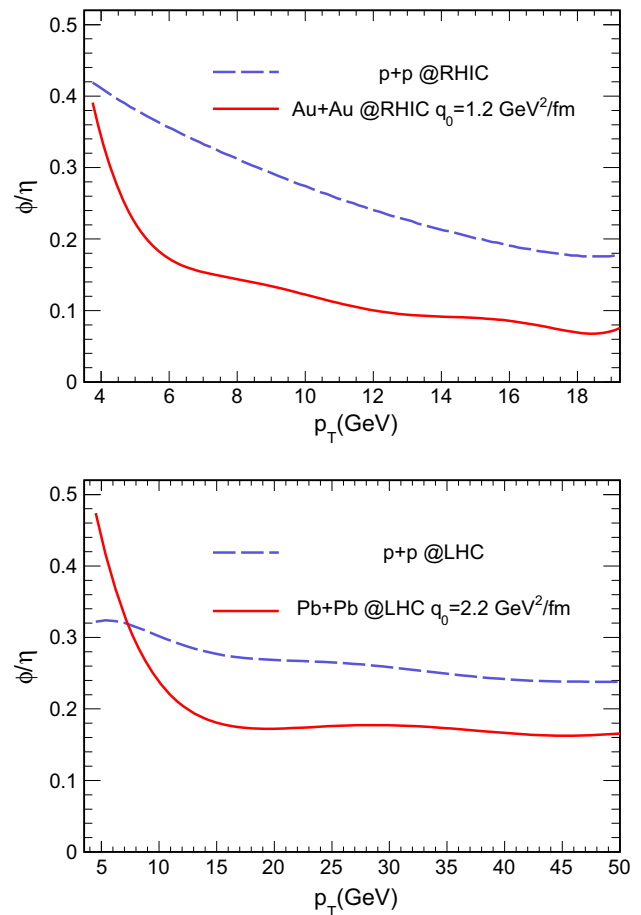


Fig. 7 Top Yield ratio ϕ/η as a function of p_T in p + p and Au + Au collisions at the at the RHIC. Bottom ϕ/η as a function of p_T in p + p and Pb + Pb collisions at the LHC

by the gluon jet. For ϕ meson production in A + A, gluon fragmentation still gives a $\sim 40\%$ contribution of the total yield in the intermediate p_T region, and $> 30\%$ at very high transverse momentum. For high transverse momentum π^0 meson production, however, because the gluon contribution fraction even in p + p is not dominant, its value in A + A collisions is further suppressed and leads to a few percent at ~ 20 GeV. A similar trend could also be observed in η and ρ^0 productions in A + A reactions.

Combining the above discussions on neutral meson productions in p + p and A + A collisions, we may reach interesting conclusions. Because at very high p_T the productions of three neutral mesons (π^0 , η and ρ^0) are all dominated by quark fragmentation, whether in p + p or A + A collisions, the yield ratios of these three neutral mesons, for example η/π^0 and ρ^0/π^0 , at very high p_T in A + A collisions will approach that in p + p reactions if quark FFs for these mesons at very high p_T have a flat dependence on z_h and the hard scale p_T , as seen in the theoretical calculations of the ratio η/π^0 in Ref. [9] and ρ^0/π^0 in Ref. [10], as well as related

experiment observation [3]. However, for the ϕ meson production, the story will be quite different: in p + p collisions the high p_T ϕ meson yield is dominated by gluon fragmentations, while in A + A reactions it should be dominated by quark fragmentation because the parton energy loss effect suppresses the relative contribution of hard gluons. Thus the yield ratios of the ϕ meson to other neutral mesons (π^0 , η and ρ^0) in A + A collisions may show different behavior with the ones in p + p reactions even at the very high p_T region.

In Fig. 6, we plot the yield ratio ϕ/π^0 as functions of p_T in p + p and A + A collisions with $\sqrt{s_{NN}} = 200$ GeV at the RHIC, and with $\sqrt{s_{NN}} = 2.76$ TeV at the LHC. In Fig. 7 and Fig. 8 we demonstrate the yield ratios ϕ/η and ϕ/ρ^0 in p + p and A + A collisions. We could observe that these three yield ratios ϕ/π^0 , ϕ/η and ϕ/ρ^0 really show distinct behavior at very high p_T in A + A collisions from the ones in p + p at both the RHIC and the LHC energies, and the distinctions are more obvious at the RHIC.

We notice that the identified leading hadron production in HIC should in general be determined by three factors: the

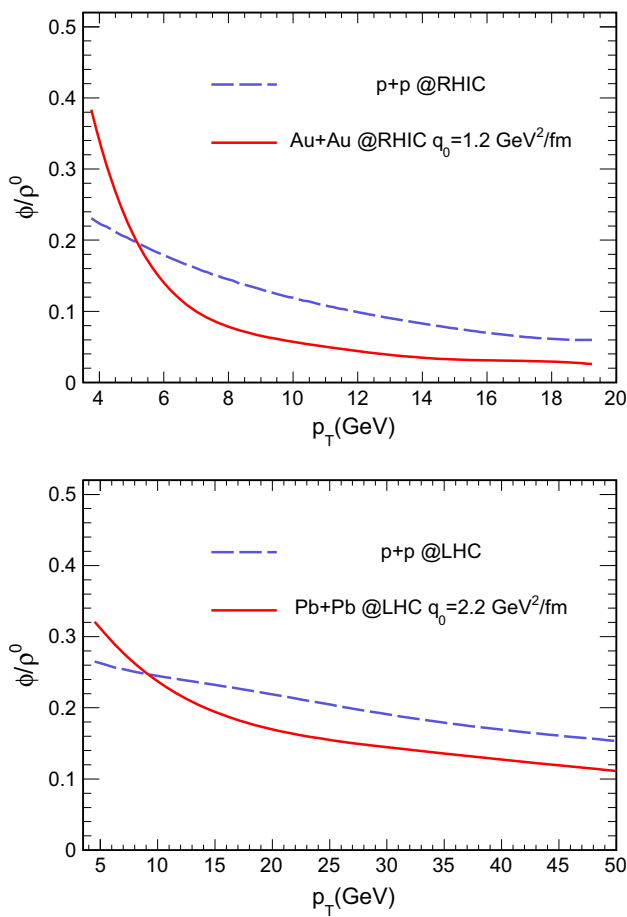


Fig. 8 Top ϕ/ρ^0 as a function of p_T in $p + p$ and $Au + Au$ collisions at the RHIC. Bottom ϕ/ρ^0 as a function of p_T in $p + p$ and $Pb + Pb$ collisions at the LHC

initial hard parton-jet spectrum, the parton energy loss mechanism, and parton FFs to the hadron in vacuum. These three factors are intertwined with each other. Even though leading hadrons in HIC are produced in the same scenario as that in which the parent parton first loses its energy in the produced QCD medium and then fragments into a leading hadron in the vacuum with the same probabilities governing high p_T hadron production in the elementary $p + p$ collisions, the high p_T yield ratios of hadrons of different species in $A + A$ may show distinct behavior from those in $p + p$ due to their inherited characteristic parton FFs. The yield ratios of ϕ/π^0 , ϕ/η and ϕ/ρ^0 discussed in this manuscript demonstrated clearly this property of the identified high p_T hadron productions in HIC.

In summary, we have provided the calculation and the theoretical prediction of the ϕ meson productions in $p + p$ and $A + A$ collisions both at the LHC and the RHIC in the framework of pQCD for the very first time. In the calculation, a higher-twist approach to the multiple scattering in the QCD medium has been used to introduce the effectively medium-modified fragmentation functions to calculate the production

of the ϕ meson in $A + A$ collisions. Due to the discovery of the gluon domination of ϕ production, which is unlike π^0 , η and ρ , we find that the calculated yield ratios of ϕ/π^0 , ϕ/ρ^0 and ϕ/η have not shown the coincidence between $A + A$ and $p + p$, which is displayed among the ratios of light quark dominated mesons: ρ^0/π^0 , η/π^0 . Therefore, the ratio of the ϕ meson to the other light quark mesons such as π^0 , η and ρ^0 , will provide an interesting probe of the color charge sensitivity of jet quenching.

Acknowledgements We thank Prof. Xin-Nian Wang for helpful discussion. This research is supported by the MOST in China under Project No. 2014CB845404, and by NSFC of China with Project Nos. 11435004, 11322546, and 11521064.

Open Access This article is distributed under the terms of the Creative Commons Attribution 4.0 International License (<http://creativecommons.org/licenses/by/4.0/>), which permits unrestricted use, distribution, and reproduction in any medium, provided you give appropriate credit to the original author(s) and the source, provide a link to the Creative Commons license, and indicate if changes were made. Funded by SCOAP³.

References

1. X.N. Wang, M. Gyulassy, Phys. Rev. Lett. **68**, 1480 (1992)
2. M. Gyulassy, I. Vitev, X.N. Wang, B.W. Zhang, In Hwa, R.C. (ed.) et al. Quark Gluon Plasma, pp. 123–191. [arXiv:nuc1-th/0302077](https://arxiv.org/abs/nuc1-th/0302077)
3. S.S. Adler et al. [PHENIX Collaboration], Phys. Rev. Lett. **96**, 202301 (2006). [arXiv:nuc1-ex/0601037](https://arxiv.org/abs/nuc1-ex/0601037)
4. A. Adare et al. [PHENIX Collaboration], Phys. Rev. D **83**, 032001 (2011). [arXiv:1009.6224](https://arxiv.org/abs/1009.6224) [hep-ex]
5. G. Agakishiev et al. [STAR Collaboration], Phys. Rev. Lett. **108**, 072302 (2012). [arXiv:1110.0579](https://arxiv.org/abs/1110.0579) [nucl-ex]
6. A. Morreale [ALICE Collaboration], [arXiv:1609.06106](https://arxiv.org/abs/1609.06106) [hep-ex]
7. X.F. Chen, C. Greiner, E. Wang, X.N. Wang, Z. Xu, Phys. Rev. C **81**, 064908 (2010). [arXiv:1002.1165](https://arxiv.org/abs/1002.1165) [nucl-th]
8. X.F. Chen, T. Hirano, E. Wang, X.N. Wang, H. Zhang, Phys. Rev. C **84**, 034902 (2011). [arXiv:1102.5614](https://arxiv.org/abs/1102.5614) [nucl-th]
9. W. Dai, X.F. Chen, B.W. Zhang, E. Wang, Phys. Lett. B **750**, 390 (2015). [arXiv:1506.00838](https://arxiv.org/abs/1506.00838) [nucl-th]
10. W. Dai, B.W. Zhang, E. Wang, [arXiv:1701.04147](https://arxiv.org/abs/1701.04147) [nucl-th]
11. H. Saveetha, D. Indumathi, S. Mitra, Int. J. Mod. Phys. A **29**(07), 1450049 (2014). [arXiv:1309.2134](https://arxiv.org/abs/1309.2134) [hep-ph]
12. D. Indumathi, H. Saveetha, Int. J. Mod. Phys. A **27**, 1250103 (2012). [arXiv:1102.5594](https://arxiv.org/abs/1102.5594) [hep-ph]
13. M. Hirai, S. Kumano, Comput. Phys. Commun. **183**, 1002 (2012). [arXiv:1106.1553](https://arxiv.org/abs/1106.1553) [hep-ph]
14. J.F. Owens, Rev. Mod. Phys. **59**, 465 (1987)
15. H.L. Lai et al. [CTEQ Collaboration], Eur. Phys. J. C **12**, 375 (2000). [arXiv:hep-ph/9903282](https://arxiv.org/abs/hep-ph/9903282)
16. A. Adare et al. [PHENIX Collaboration], Phys. Rev. C **83**, 024909 (2011). doi:10.1103/PhysRevC.83.024909, [arXiv:1004.3532](https://arxiv.org/abs/1004.3532) [nucl-ex]
17. T. Richer [ALICE Collaboration], [arXiv:1505.04717](https://arxiv.org/abs/1505.04717) [hep-ex]
18. J. Adam et al. [ALICE Collaboration], [arXiv:1702.00555](https://arxiv.org/abs/1702.00555) [nucl-ex]
19. D.G. d'Enterria, [arXiv:nuc1-ex/0302016](https://arxiv.org/abs/nuc1-ex/0302016)
20. X.F. Guo, X.N. Wang, Phys. Rev. Lett. **85**, 3591 (2000). [arXiv:hep-ph/0005044](https://arxiv.org/abs/hep-ph/0005044)
21. X.N. Wang, X.F. Guo, Nucl. Phys. A **696**, 788 (2001). [arXiv:hep-ph/0102230](https://arxiv.org/abs/hep-ph/0102230)

22. B.W. Zhang, X.N. Wang, Nucl. Phys. A **720**, 429 (2003). [arXiv:hep-ph/0301195](#)
23. B.W. Zhang, E. Wang, X.N. Wang, Phys. Rev. Lett. **93**, 072301 (2004). [arXiv:nucl-th/0309040](#)
24. A. Schafer, X.N. Wang, B.W. Zhang, Nucl. Phys. A **793**, 128 (2007). [arXiv:0704.0106](#) [hep-ph]
25. Z.Q. Liu, H. Zhang, B.W. Zhang, E. Wang, Eur. Phys. J. C **76**(1), 20 (2016). [arXiv:1506.02840](#) [nucl-th]
26. T. Hirano, Phys. Rev. C **65**, 011901 (2002)
27. T. Hirano, K. Tsuda, Phys. Rev. C **66**, 054905 (2002)
28. K.J. Eskola, H. Paukkunen, C.A. Salgado, JHEP **0904**, 065 (2009). [arXiv:0902.4154](#) [hep-ph]
29. K.M. Burke et al. [JET Collaboration], Phys. Rev. C **90**(1), 014909 (2014). doi:[10.1103/PhysRevC.90.014909](#), [arXiv:1312.5003](#) [nucl-th]